Available online at www.sciencedirect.com
SCIENCE DIRECT®
Physica A 338 (2004) 493–510
PHYSICA A
www.elsevier.com/locate/physa

Lattice-gas modeling of enantioselective adsorption by template chiral substrates

F. Romá[a], D. Stacchiola[b], W.T. Tysoe[b], G. Zgrablich[c,*,1]

[a] *Laboratorio de Ciencias de Superficies y Medios Porosos, Universidad Nacional de San Luis, San Luis, Argentina*
[b] *Department of Chemistry, University of Wisconsin, Milwaukee, USA*
[c] *Departamento de Química, Universidad Autónoma Metropolitana, Iztapalapa, P.O. Box 55-534, Mexico DF, Mexico*

Received 4 December 2003

Abstract

The general behavior of enantioselective adsorption by templated chiral substrates is studied in the framework of lattice-gas and random sequential adsorption theories. The template is assumed to be formed by randomly preadsorbing a chiral species A on a square lattice of sites. A second chiral probe species, B, thus performs a random sequential adsorption process on the templated substrate and the enantioselectivity of the process with respect to one of the B enantiomers is obtained as a function of the relevant parameters of the model. All species considered in the present study are considered as monomers, i.e., they occupy a single adsorption site. In an extension of the simple model, the possibility that the chiral probe species can themselves act as templates is taken into account.

It is shown how different arrangements of A molecules on the surface generate different enantioselectivities as a function of coverage, some of which have been observed experimentally.

PACS: 82.20.Hf; 82.20.Wt; 82.65.Jv

Keywords: Chiral catalysis; Enantioselectivity; Adsorption

1. Introduction

The term chirality, first coined by Lord Kelvin in 1893, refers to the property by which the mirror image (mathematically obtained by an inversion transformation) of

* Corresponding author.
E-mail address: giorgiozgrablich942@hotmail.com (G. Zgrablich).

[1] On Sabbatical Leave from Laboratorio de Ciencias de Superficies y Medios Porosos, Universidad Nacional de San Luis.

0378-4371/$ - see front matter
doi:10.1016/j.physa.2004.03.024

a geometrical figure cannot be brought into coincidence with itself. Molecules having chirality, or chiral molecules, are found in two forms, enantiomers, each being the mirror image of the other, but which are not superimposable. Often the two enantiomers, R and S, of a chiral molecule have different chemical and physical properties, despite having the same chemical composition. This is of fundamental importance in drug design, since it has been found that, while one enantiomer of a drug may be completely effective, the other can be very harmful. Thus, understanding of enantioselective processes is therefore important for drug synthesis where one of the two enantiomers of a chiral molecule must be selectively produced.

There are currently thought to be two main mechanisms by which a chiral modifier imparts enantioselectivity to a heterogeneous catalyst

(a) *One-to-one mechanism*: One chiral modifier is anchored to a surface in such a way it modifies an adjacent site to impart enantioselectivity to the adsorption of a reactant molecule. This kind of mechanism may operate in the case of large chiral modifiers, such as cinchonidine [1–10].
(b) *Template mechanism*: In this case the substrate is partially covered by a modifier of a given chirality, say R. Some configuration of these around a vacant site forms an "enantioselective pockets". In other words, this assembly of A species will selectively affect the subsequent adsorption of a mixture of probe chiral molecules. This kind of mechanism appears to apply to the system studied in Refs. [11–20].

Given that the precise structural relationship between a templating overlayer and the probe molecules is not yet well understood, advances in the study of the problem can be made by taking advantage of the fact that the two mechanisms described above should yield completely different dependences of enantioselectivity as a function of coverage of the chiral one-to-one modifier, or templating species. Catalytic systems leading to enantioselectivity [21,22], based on the modification of the substrate by chemisorption of a templating chiral species, seem to yield a significant enantioselective excess, but only in a narrow range of coverage of the templating species [23–25]. A similar effect has been found in ultrahigh vacuum experiments [19] for the enantioselective chemisorption of propylene oxide on a Pd(1 1 1) surface that was chirally templated by 2-butoxide species. It was found [20] that this behavior could be explained by assuming a template mechanism, such as that described in section (b) above.

In the present study, we focus on understanding how enantioselectivity depends on coverage for templating mechanism, based on a lattice-gas model, and to explore the effects of several parameters to provide a framework for analyzing experimental data. To achieve this, we initially use a relatively simple model where both the template and probe species adsorb as monomers (therefore occupying a single adsorption site) on a square lattice of sites and where no lateral interactions are present among chemisorbed molecules. Future work will extend the theory to examining interacting species, multi-site adsorption and other lattice geometries. In Section 2, we outline the simplified model, and derive the general equations governing the enantioselective adsorption in the case that only template (A) molecules affect the adsorption of probe (B) molecules (Section 3). Results are presented and discussed in Section 4. Since the

template-covered surface is subsequently exposed to a chiral probe, it may be that the probe molecules themselves, once absorbed, can affect the subsequent adsorption probe molecules. That is, the probe molecules on a templated surface may themselves act as a template. A discussion of this effect is given in Section 5.

The predictions of these models are in good general agreement with the behavior observed for enantioselective chemisorption on templated surfaces in ultrahigh vacuum [19] in the sense that, in both cases, enantioselectivity is only found over a relatively narrow coverage range. However, since detailed adsorption geometries and sites are not yet available for the experimental systems, a closer comparison between experiment and theory is not, at this stage, possible. Rather the goal of this work is to provide relatively simple analytical expressions for subsequent comparison with experimental data as these become available.

2. Description of the simplified model

We consider two chiral species, species A, a template, and species B, a probe. Both consist of enantiomers of two kinds, R and S. The substrate is taken to be a two-dimensional square lattice of sites. Each molecule adsorbs as a monomer, occupying only a single site, and each site can accommodate only one molecule, so that only adsorption into the first layer it considered. The theoretical analysis consists of two stages

Stage 1: A given coverage, θ_A, of the template molecules A is established through a sequential irreversible random adsorption [26,27] of a mixture of A_R and A_S enantiomers, f_{AR} being the fraction of R enantiomers and $1-f_{AR}$ that of S enantiomers in the impinging flux. The functional dependence on f_{AR} is important in heterogeneous enantioselective catalysis where an initially racemic mixture ($f_{AR}=0.5$) reacts enantioselectively, such that one of the enantiomers is preferentially removed resulting in a time-dependent behavior of f_{AR}.

Stage 2: B molecules are adsorbed in a sequential irreversible random process on vacant sites left after Stage 1 is completed. This process can be executed in two different ways:

(a) *Simultaneous adsorption*: The surface is exposed to a flux consisting of a mixture of B_R and B_S species, f_{BR} being the fraction of R enantiomers and $1-f_{BR}$ that of S enantiomers, until saturation. This mimics the process occurring during a catalytic reaction.
(b) *Sequential adsorption*: The surface is exposed first to a flux of one of the B species, say B_R, until saturation. The surface is then cleaned of probe molecules and the adsorption process is repeated with a flux of the other B species, say B_S. This mimics the protocol that is used in ultrahigh vacuum experiments [19].

As seen below, this leads to two different values of the enantioselectivity. The model assumes that *selectivity* towards a given B enantiomer is caused by the presence of a particular number and arrangement of chiral A templates around a vacant site at

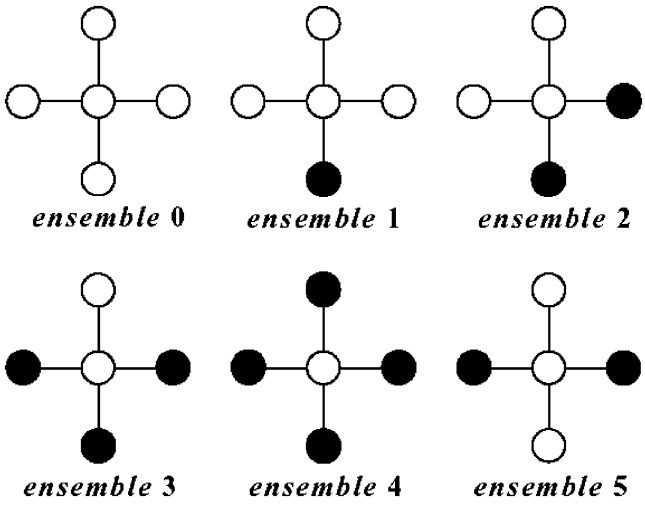

Fig. 1. Selective ensembles around a site where a B enantiomer can adsorb (central site). The number under each diagram characterizes the type of ensemble.

which the B molecule can adsorb, while the same arrangement of A enantiomers of the opposite kind will cause an *anti-selective* effect. Any other arrangement will be *enantioneutral*. Such information on the number of chiral template species that are required to provide an enantioselective reaction site is central to fundamentally understanding the requirements for the formation of heterogeneous chiral catalysts.

In the simplified model presented below, the presence of other previously adsorbed B particles around the vacant site is assumed to be irrelevant to its selectivity towards the incoming B particle. Once the template coverage has been established, any central vacant site can be classified into one of the 6 ensembles shown in Fig. 1, referred to as *ensemble* 0, 1,…, 5, where the filled circles represent an adsorbed A (template) molecule (either an R or an S). We will explore the enantioselectivity towards B molecules when any one of the 6 ensembles is chosen as an *enantioselective ensemble*.

To more easily understand the proposed selectivity mechanism, we will illustrate it with an example. Suppose that only ensemble 2 is enantioselective, then configurations (a) and (b) shown in Fig. 2 will have a net *selective* effect on a B_R species adsorbing on the central site. In fact, in both configurations, A_R adsorbed species (indicated simply as R in the figure) form an ensemble 2, which is the selector, while A_S species (indicated as S) form an ensemble 0 in (a) and an ensemble 1 in (b), both being *neutral*. On the other hand, following similar arguments, configurations (c) and (d) will have a net *anti-selective* effect on the adsorption of B_R species. A completely symmetric situation is considered for adsorption of B_S species.

In order to describe the different possibilities, two parameters are introduced: $0 < s \leqslant 1$, the probability of adsorption on a non-enantioselective site, and $0.5 < q \leqslant 1$, as the adsorption probability on a selective one (thus $1 - q$ will be the probability

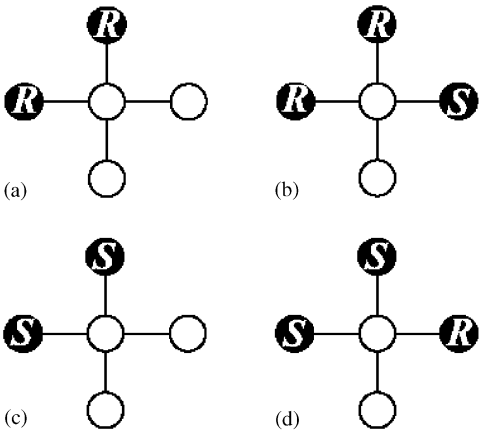

Fig. 2. Examples of ensembles where $R(S)$ stands for an adsorbed $A_R(A_S)$ species. Assuming that ensemble 2 is the selective one, then ensembles (a) and (b) have a net selective effect for the adsorption of a B_R species, while ensembles (c) and (d) have a net anti-selective effect.

Table 1
Selectivity rules

Ensemble A_R	Ensemble A_S	Net effect	Adsorption probability
(a) *Adsorption of* B_R			
Selective	Selective	Neutral	s
Neutral	Neutral	Neutral	s
Selective	Neutral	Selective	q
Neutral	Selective	Antiselective	$1-q$
(b) *Adsorption of* B_S			
Selective	Selective	Neutral	s
Neutral	Neutral	Neutral	s
Neutral	Selective	Selective	q
Selective	Neutral	Antiselective	$1-q$

of adsorption on an anti-selective site). Table 1(a) and (b) summarizes all possible situations for the adsorption of B_R and B_S species, respectively.

The present model is necessarily geometrical for two reasons. Firstly, as already mentioned, detailed structural information on the nature of heterogeneous enantioselective sites is still unavailable. Secondly, as will be shown below, enantioselectivity should be a "yes-or-no" action in order to explain the behavior observed experimentally in Ref. [19]; if we were to attribute the enantioselective action to some sort of interaction among A_R and B_R and B_S species, then for the *sequential adsorption* experiment there would be no enantioselectivity. This is because both B_R and subsequently B_S, would eventually achieve the saturation coverage $1-\theta_A$.

In summary, the proposed model has three external parameters, θ_A, f_{AR} and f_{BR}, and three internal parameters determining the adsorption dynamics, s, q, and the index i identifying the selective ensemble. In the following Section, we derive the general equations describing the process.

3. Analytical theory

3.1. Simultaneous adsorption

We first derive the exact analytical equations for the case where B_R and B_S species adsorb simultaneously on an A-templated substrate.

After Stage 1 (coverage of the surface by the template) is complete, the total number of adsorbed particles, N, at time t (taking $t = 0$ as the beginning of Stage 2) will be

$$N = N_A + N_R + N_S \ , \tag{1}$$

where N_A is the total number of adsorbed A molecules (either A_R or A_S), which remains constant, and N_R (N_S) is the number of adsorbed B_R (B_S) species. If M is the total number of adsorbing sites in the lattice, then the corresponding equation for coverage is

$$\frac{N}{M} = \theta = \theta_A + \theta_R + \theta_S \ . \tag{2}$$

If F_B is the flux of B molecules arriving at the surface, then

$$F_B = F_R + F_S \ , \tag{3}$$

where F_R (F_S) is the flux of B_R (B_S) molecules. In a differential time $\mathrm{d}t$ we have

$$\mathrm{d}F_B = M\,\mathrm{d}t, \quad \mathrm{d}F_R = f_{BR}M\,\mathrm{d}t, \quad \mathrm{d}F_S = (1 - f_{BR})M\,\mathrm{d}t \ . \tag{4}$$

Stage 2 is complete when the surface is saturated, so that when $t \to \infty$

$$1 = \theta_A + \Theta_R + \Theta_S \ , \tag{5}$$

where Θ stands for the maximum coverage for each species at saturation.

Now, let $P_{R,s}$, $P_{R,a}$, and $P_{R,n}$ be the conditional probabilities that, after impinging on a vacant site, a molecule B_R experiences a net selective, anti-selective, or neutral ensemble, respectively. Similar quantities $P_{S,s}$, $P_{S,a}$ and $P_{S,n}$ are defined for species B_S. However, it is evident that

$$P_{R,s} = P_{S,a}, \quad P_{R,a} = P_{S,s}, \quad P_{R,n} = P_{S,n} \ . \tag{6}$$

With these probabilities, the fraction of vacant sites at $t = 0$, ϕ, belonging to an ensemble with a given net effect for the adsorption of B_R is obtained as

$$\phi_{R,s} = (1 - \theta_A)P_{R,s}, \quad \phi_{R,a} = (1 - \theta_A)P_{R,a}, \quad \phi_{R,n} = (1 - \theta_A)P_{R,n} \ . \tag{7}$$

We also define the number of adsorbed B_R species on sites belonging to an ensemble with a given net enantioselective effect as $N_{R,s}$, $N_{R,a}$, and $N_{R,n}$, and the corresponding

coverages $\theta_{R,s}$, $\theta_{R,a}$, and $\theta_{R,n}$. Similar definitions and equations hold for the adsorption of B_S species.

We can now easily write the master equation for the adsorption of B_R species on vacant sites belonging to an ensemble with a net selective effect

$$\mathrm{d}N_{R,s} = q(\phi_{R,s} - \theta_{R,s} - \theta_{S,a})\,\mathrm{d}F_R \ . \tag{8}$$

Taking Eq. (4) into account Eq. (8) can be rewritten as

$$\frac{1}{q f_{BR}} \frac{\mathrm{d}\theta_{R,s}}{\mathrm{d}t} = \phi_{R,s} - \theta_{R,s} - \theta_{S,a} \ . \tag{9}$$

Following the same arguments for the adsorption of B_S species on net anti-selective sites, we have

$$\frac{1}{(1-q)(1-f_{BR})} \frac{\mathrm{d}\theta_{S,a}}{\mathrm{d}t} = \phi_{S,a} - \theta_{S,a} - \theta_{R,s} \ . \tag{10}$$

Given that $\phi_{S,a}=\phi_{R,s}$, from Eqs. (9) and (10) we obtain the following relation between the maximum coverages at saturation $\Theta_{R,s}$ and $\Theta_{S,a}$:

$$\Theta_{R,s} = \frac{q f_{BR}}{(1-q)(1-f_{BR})} \Theta_{S,a} \ . \tag{11}$$

In order to obtain the two maximum coverages separately we make use of the relation

$$\phi_{R,s} = \Theta_{R,s} + \Theta_{S,a} \ . \tag{12}$$

Then, from Eqs. (11) and (12), and taking into account Eq. (7), we get

$$\Theta_{R,s} = \frac{q f_{BR}(1-\theta_A)P_{R,s}}{(1-q) + f_{BR}(2q-1)} \ , \tag{13}$$

$$\Theta_{S,a} = \frac{(1-q)(1-f_{BR})(1-\theta_A)P_{R,s}}{(1-q) + f_{BR}(2q-1)} \ . \tag{14}$$

Following a similar scheme, we can write the remainder of maximum coverages as

$$\Theta_{R,a} = \frac{(1-q) f_{BR}(1-\theta_A)P_{R,a}}{q - f_{BR}(2q-1)} \ , \tag{15}$$

$$\Theta_{S,s} = \frac{q(1-f_{BR})(1-\theta_A)P_{R,a}}{q - f_{BR}(2q-1)} \ , \tag{16}$$

$$\Theta_{R,n} = f_{BR}(1-\theta_A)P_{R,n} \ , \tag{17}$$

$$\Theta_{S,n} = (1-f_{BR})(1-\theta_A)P_{R,n} \ . \tag{18}$$

Now, from Eqs. (13) to (18), the selectivity for *simultaneous* adsorption, α_i, onto ensemble i ($i = 0, 1, 2, 3, 4, 5$) can be calculated explicitly as

$$\alpha_i = \frac{f_{BR}}{(1 - f_{BR})} \left\{ \frac{\frac{qP_{R,s,i}}{(1-q)+f_{BR}(2q-1)} + \frac{(1-q)P_{R,a,i}}{q-f_{BR}(2q-1)} + P_{R,n,i}}{\frac{qP_{R,a,i}}{q-f_{BR}(2q-1)} + \frac{(1-q)P_{R,s,i}}{(1-q)+f_{BR}(2q-1)} + P_{R,n,i}} \right\} , \tag{19}$$

where a sub index i has been added to the probabilities P to stress the fact that they depend upon the chosen selective ensemble (see Fig. 1). With the above definition there is a positive selectivity towards A_R when $\alpha_i > 1$.

3.2. Sequential adsorption

In the case where species B_R and B_S are adsorbed sequentially on the templated surface, the parameter q must equal unity in order to have an enantioselectivity greater than 1. In fact, exposing the template surface after Stage 1 to a flux of B_R species, all sites belonging to a neutral ensemble or to a selective ensemble will be completely filled. The same will occur when the templated surface is exposed to a flux of B_S species. An important consequence of this property is that, if the behavior observed experimentally in Ref. [19] is to be described, the selectivity must be a "yes-or-no" action.

With $q = 1$, it can be seen that

$$\Theta_R = (1 - \theta_A)P_{R,n} + (1 - \theta_A)P_{R,s}, \quad \Theta_S = (1 - \theta_A)P_{S,n} + (1 - \theta_A)P_{S,s} . \tag{20}$$

Then, taking into account Eq. (6), the enantioselectivity of ensemble i for sequential adsorption, β_i, is given by

$$\beta_i = \frac{P_{R,n,i} + P_{R,s,i}}{P_{R,n,i} + P_{R,a,i}} . \tag{21}$$

3.3. General remarks

Eqs. (19) and (21) determine the enantioselectivity for simultaneous and sequential adsorption, respectively, of the two enantiomers of the probe molecule B in terms of the probabilities P. The derivation of the probabilities for each selective ensemble is shown in the appendix.

The enantioselectivity α (Eq. (19)) depends on all external parameters, θ_A, f_{AR} and f_{BR}. In fact, even if f_{AR} does not appear explicitly in the equation, the probabilities P depend on this quantity. Note that the enantioselectivity β (Eq. (21)) does not depend on the external parameter f_{BR} since adsorption is carried out sequentially with pure B_R and pure B_S species. On the other hand, α depends only on two internal parameters, q and i (the type of selective ensemble chosen), while β depends only on the single internal parameter i. Both selectivities do not depend on the internal parameter s in the simplified model considered in this Section. In fact, in this case, the effect of s is simply to retard the adsorption on neutral sites. However, the parameter s will certainly play a role in the extended model to be presented in Section 5.

4. Results for the selectivity in the simplified model

We now explore the influence of the different parameters on the enantioselectivity. In all figures symbols represent the results of Monte Carlo simulations [28], which were performed to corroborate the analytical theory, while lines represent the predictions of equations derived in Section 3.

The enantioselectivity was calculated for simultaneous adsorption onto each of the six selective ensembles as a function of A coverage, for fixed $f_{AR} = 1$ and $f_{BR} = 0.5$ and for different values of q. Thus, in this case the template has been formed with pure A_R and a racemic mixture of chiral probe molecules is incident on the surface. This has been explored previously [20] and the Monte Carlo simulations reproduced the analytical theory extremely well. In this case, the effect of parameter q is simply to uniformly reduce the enantioselectivity, as expected, with no additional effects (peak shifting, for example). Given this, and the fact that a "yes-or-no" action must be considered for sequential adsorption, only the value $q = 1$ will be considered from now on. It was found that the different geometrical arrangements of template species produce different enantioselectivities depending on the coverage. An important feature is that only ensembles 1, 2, 3 and 5 show relatively sharp maxima, in accord with experimental observations in catalytic and UHV systems. In particular, ensemble 1 gives a maximum located approximately at $\theta_A = 0.25$, resembling the behavior observed in the ultrahigh vacuum chemisorption experiments of Ref. [19].

Fig. 3 shows the effect of f_{AR}, the composition of the flux of template species during Stage 1, while the composition of the flux of probe molecules is maintained at f_{BR}=0.5, for $q = 1$, in the case of simultaneous adsorption. Two new interesting features are observed: (a) ensembles 2, 3 and 5 present a quite noticeable shift in the position of the maximum toward higher A coverage as f_{AR} decreases, while for ensemble 1 the shift is much smaller, and in the opposite direction; (b) for ensemble 1 the enantioselectivity is reversed toward B_S for sufficiently high θ_A when $f_{AR} < 1$. These features may serve as a clue for experimentally determining which of the templating ensembles is selective.

A very similar behavior is found in the case of sequential adsorption of B enantiomers with the only difference being that the enantioselectivity is lower than in the case of simultaneous adsorption.

We now focus on the effect of f_{BR}, the composition of the flux of probe species, for $f_{AR} = 1$ and $q = 1$, in Fig. 4. As can be seen, it is possible to enrich a given mixture of B enantiomers through some of the enantioselective ensembles. Thus, suppose a selective ensemble i gives a maximum selectivity $\alpha_{i,m}$ for a given coverage θ_A with a given initial composition f_{BR}. Then, after Stage 2 is completed, the new composition will be

$$f_{BR}^{*} = \frac{\Theta_{BR}}{\Theta_{BR} + \Theta_{BS}} = \frac{\alpha_{i,m}}{\alpha_{i,m} + 1} \,. \tag{22}$$

Then, if, for example, a flux of probe molecules with a composition $f_{BR} = 0.25$ is incident on a template surface whose selective ensemble is ensemble 2, we see

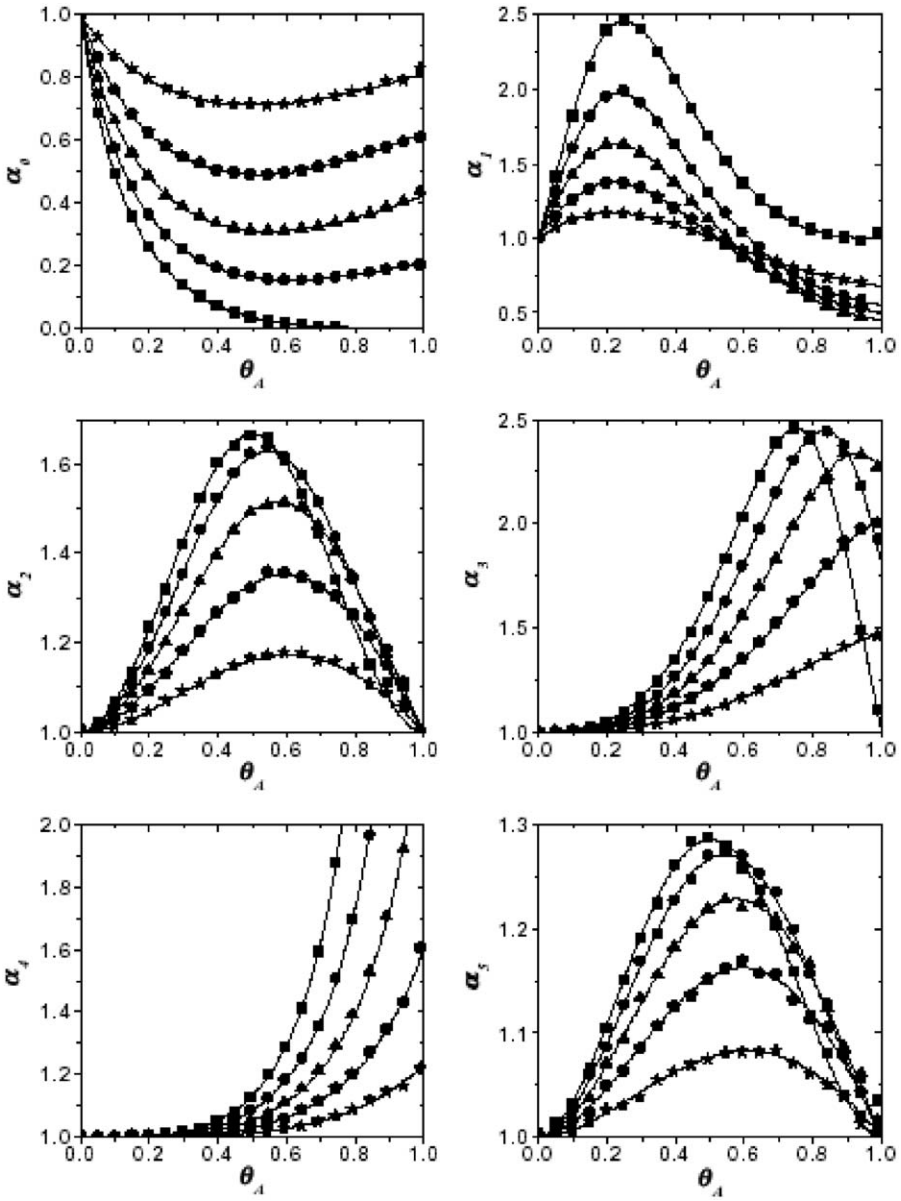

Fig. 3. Selectivity for the simultaneous adsorption process for fixed $q = 1.0$ and $f_{BR} = 0.5$ and for different values of f_{AR}: squares, $f_{AR}=1.0$; circles, $f_{AR}=0.9$; triangles, $f_{AR}=0.8$; pentagons, $f_{AR}=0.7$; stars, $f_{AR}=0.6$.

from Fig. 4 that the maximum enantioselectivity is approximately $\frac{7}{9}$. Then, by Eq. (22), when Stage 2 is completed we have a new composition $f^*_{BR} = 0.437$, which is substantially larger than the initial fraction. By repeating the procedure

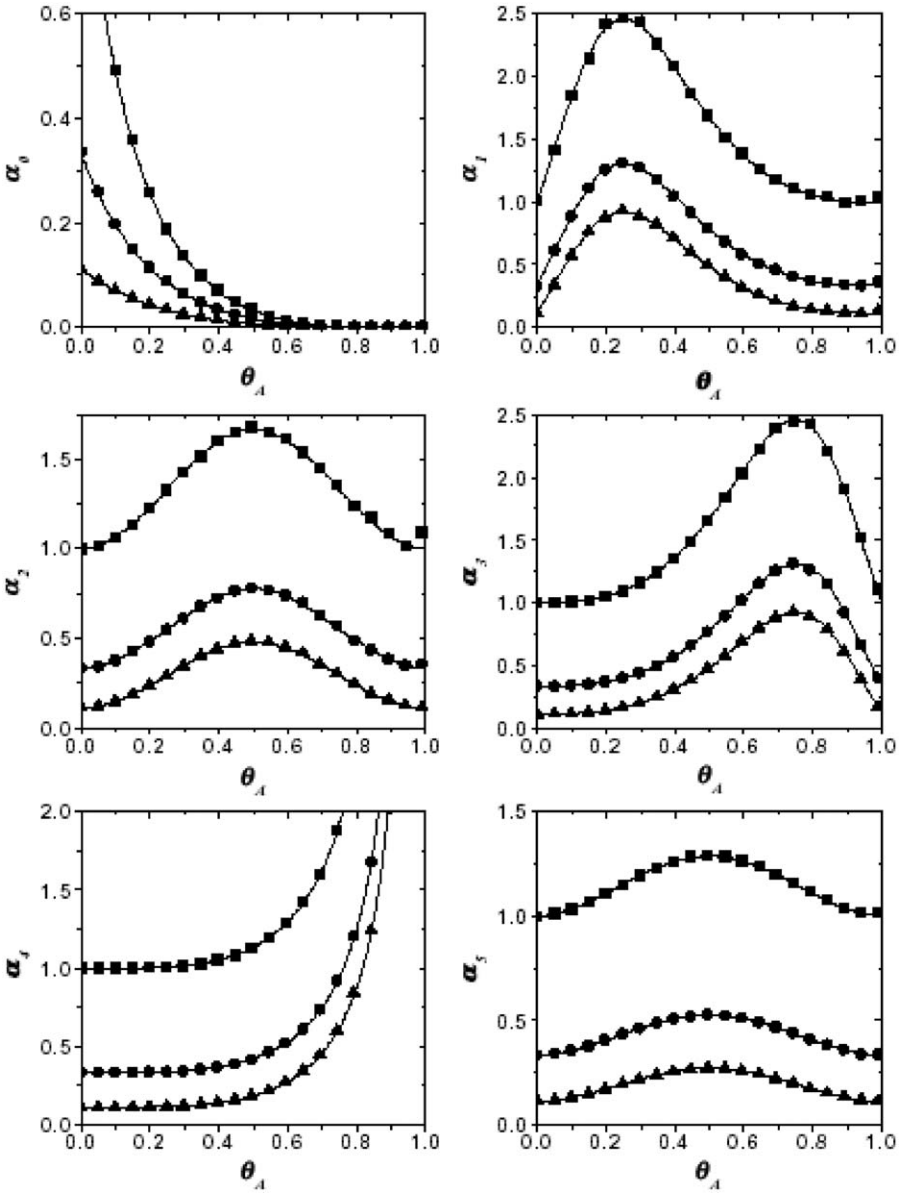

Fig. 4. Selectivity for the simultaneous adsorption process for fixed $q = 1.0$ and $f_{AR} = 1.0$ and for different values of f_{BR}: squares, $f_{BR} = 0.5$; circles, $f_{BR} = 0.25$; triangles, $f_{BR} = 0.1$.

several times the mixture of B molecules would become enriched with enantiomer B_R. Such processes occur during chiral separation processes such as chromatography.

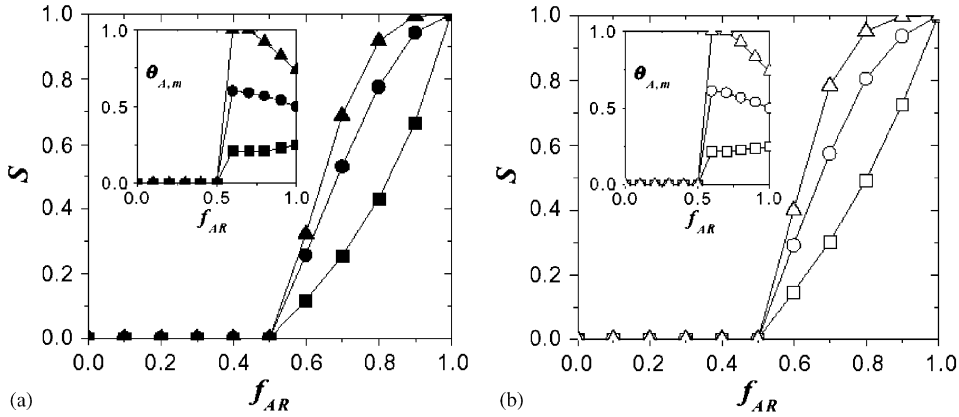

Fig. 5. Normalized selectivity and location of maxima for fixed $q = 1.0$ and $f_{BR} = 0.5$: for simultaneous adsorption (black symbols(a)) and sequential adsorption (open symbols(b)), and for ensembles 1 (squares), 2 (circles) and 3 (triangles).

The location, $\theta_{A,m}$, and value of the maximum in selectivity can be found directly from exact solutions, Eqs. (19) and (21). We now define a *normalized selectivity*, S as

$$S_i = \frac{\alpha_{i,m} - 1}{\alpha_{i,m,1} - 1} , \tag{23}$$

where $\alpha_{i,m,1}$ is the value of the maximum selectivity corresponding to $f_{AR}=1$. The same definition can be applied to the selectivity β corresponding to sequential adsorption of probe enantiomers. The behavior of normalized selectivities and the location of maxima are shown in Fig. 5, for both simultaneous (black symbols) and sequential (open symbols) adsorption, for those ensembles presenting a maximum in selectivity as a function of f_{AR}. As mentioned above, this behavior can provide experimental clues to which ensemble is enantioselective in a given system.

5. Extended model

In order to extend the basic model to more general situations, a substantial modification in Stage 2 is introduced: it is now assumed that adsorbed B enantiomers can also contribute to the enantioselectivity with the same rules as before. That is, this takes account of the fact that the adsorption of chiral probe (B) molecules may affect the enantioselectivity of molecules that subsequently adsorb onto the surface. More specifically, adsorbed B_R and B_S species will behave just as templating species A_R and A_S, respectively, for new B enantiomers impinging on the surface. R and S enantiomers (either A or B) are assumed to form identical ensembles to those defined in the basic model, and the sticking probabilities on an empty central site belonging to these ensembles are given by the same rules as in Tables 1(a) and (b), except that

now ensembles A_R and A_S should be thought as the more general ensembles R and S, respectively. This more complex situation cannot be treated analytically and is explored using Monte Carlo simulations. In the same way as in the basic model, Stage 2 can be accomplished in two ways: simultaneous and sequential adsorption of probe enantiomers. As before, the effect of parameter q is merely to uniformly decrease the enantioselectivity, with no other effects, and the results are not shown here.

Fig. 6 shows the effect of parameter f_{AR} for fixed $q = 1$ and $f_{BR} = 0.5$, in the case of simultaneous adsorption of B enantiomers. The symbols represent the simulation results for the extended model and they are compared with the exact results for the basic model (solid lines). The new features are that ensemble 1 no longer exhibits a maximum in selectivity and that, in those ensembles presenting a maximum, the peaks are shifted to lower values of θ_A. Results presented here correspond to $s = 1$, however contrary to what was found for the basic model, enantioselectivity *does* now depend on the value of s. The effect of this parameter, the probability of adsorption on vacant sites belonging to a neutral ensemble, is that of uniformly increasing the enantioselectivity as s decreases, as expected, with no additional effects, so that the dependence on s will not be shown.

The effect of the same parameters, but for the case of sequential adsorption of B enantiomers, is shown in Fig. 7. It is interesting to note that, for ensembles 2 and 5, the peaks are now shifted to the right compared to the results of the basic model, while for ensembles 3 and 4 the results for both models are practically identical. This is due to the fact that, in these particular cases, adsorbed B particles cannot change a net enantioselective or neutral ensemble into a net anti-selective one, and vice versa. However, they can change a neutral ensemble into an enantioselective one, but this does not affect the selectivity for sequential adsorption.

Finally, by varying f_{BR} for fixed $q = 1$, $f_{AR} = 1$ and $s = 1$, the same effect as that found for the basic model, concerning the possibility of enrichment of a B mixture, is also observed in this case.

As noted above, it is not possible to make precise comparisons between experiment and theory because of the lack of precise structural information in the latter case. However, as also emphasized above, the general behavior found for enantioselective chemisorption of propylene oxide on a 2-butoxide-templated Pd(1 1 1) surface [19] is in general agreement with the behavior found theoretically. In the particular case of sequential exposure to the probe molecule B, we find that selectivity must be considered as a "yes-or-no" action ($q = 1$). The selective ensemble producing a behavior in *qualitative* agreement with experimental results is ensemble 1 (Fig. 1) and the correspondence between the experimental and theoretical behavior is illustrated in Fig. 8. Further, more detailed comparisons must await additional results on the experimental geometries.

6. Conclusions

We have described a statistical strategy for studying the behavior of the enantioselective adsorption of probe chiral species on chirally templated substrates, motivated

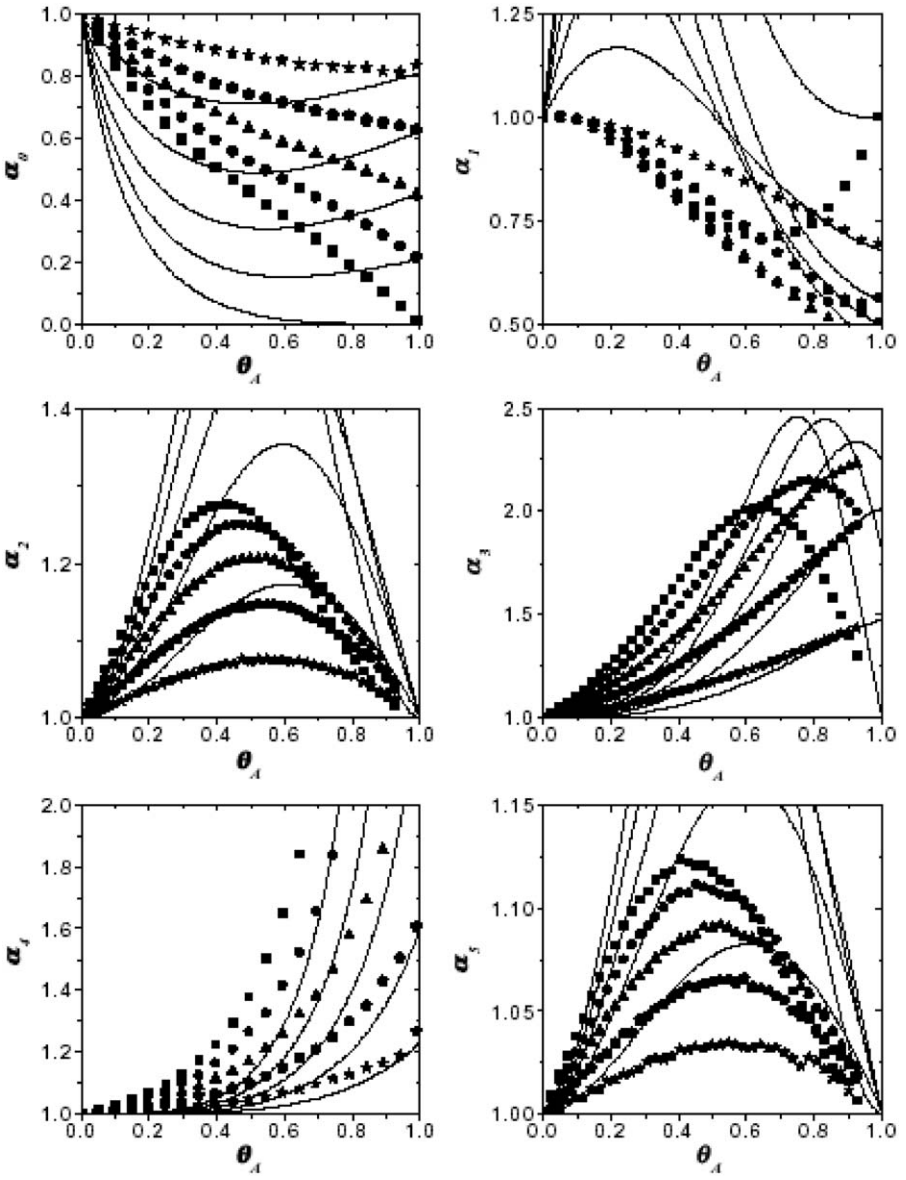

Fig. 6. Selectivity for the simultaneous adsorption process: comparison between the extended model (symbols) and the simplified model (full lines). Symbols are the same as those in Fig. 3.

by experimental results obtained both in catalytic and UHV systems. Without claiming that the proposed theory is the only way to explain the fact that a high enantioselectivity is observed only over a narrow coverage range of template molecules, we consider

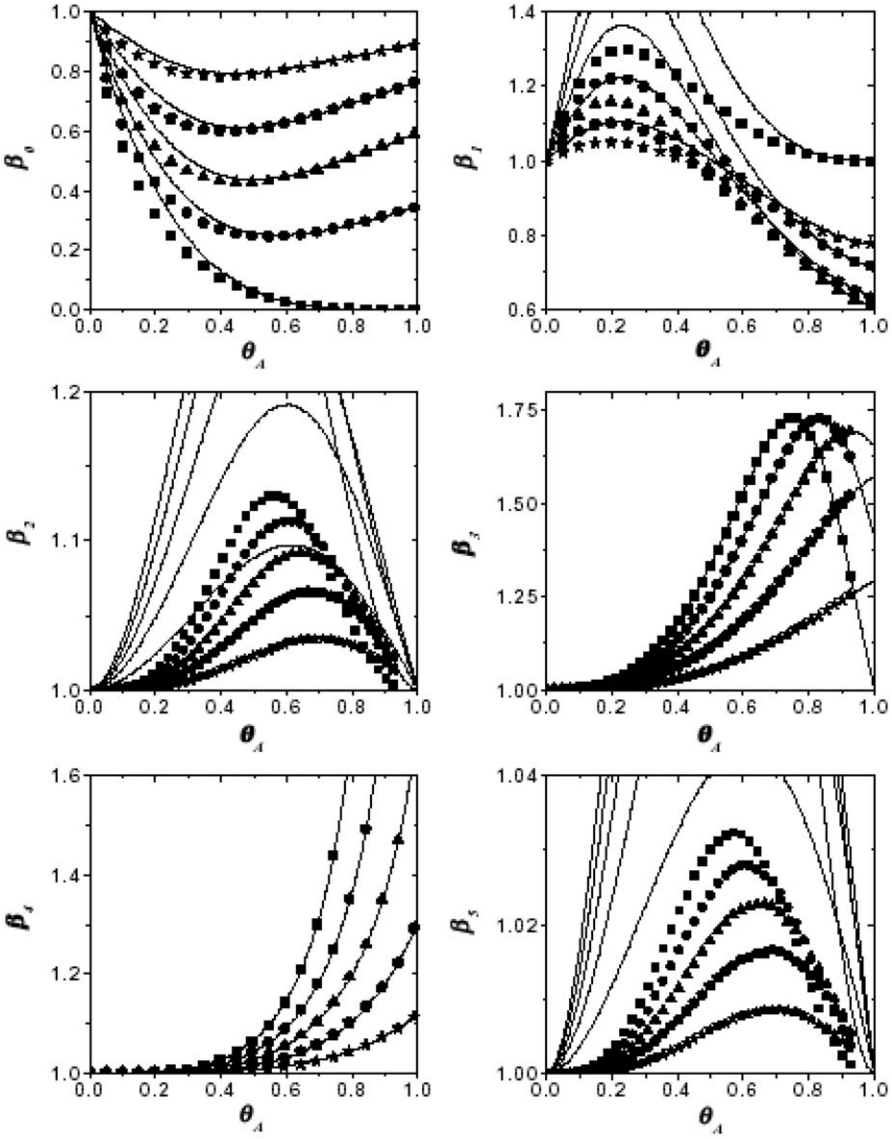

Fig. 7. Selectivity for the sequential adsorption process, comparison between the extended model (symbols) and the simplified model (full lines). Symbols are the same as those in Fig. 3.

the present study to be a first step for more deeply understanding the process. Other effects such as geometry changes of the chiral modifier as a function of coverage may also contribute. However, we have discovered that only some of the possible selective ensembles will lead to a behavior similar to that observed experimentally and

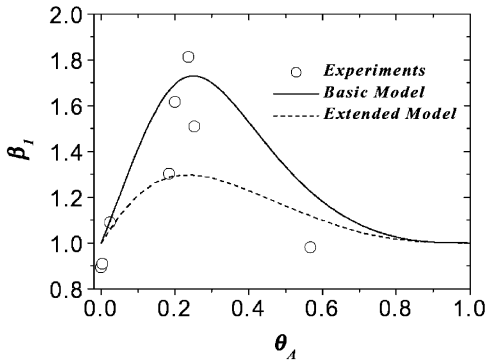

Fig. 8. Comparison between experimental data of Ref. [19] and model predictions for $q = 1$, $f_{AR} = 1$, and $i = 1$, showing that ensemble 1 gives the correct maximum selectivity for both the simplified and extended model.

have explored the influence of the relevant parameters. In particular, our results will be useful in designing experiments with the aim of discovering which ensemble is selective for a given system. Of course, this could be obscured by the possibility that in a given system more than one ensemble contributes to the enantioselectivity. In that case, the observed enantioselectivity would be a superposition of the enantioselectivities of each of the contributing ensembles.

Extensions of the models presented here, which assume that the template is obtained by random adsorption of A species on a square lattice in Stage 1, can be achieved by introducing lateral interactions amongst A species in such a way that they are forced to form more organized patterns. Other modifications could be developed by considering other kinds of (for example, triangular) lattices and by using molecules than can adsorb onto more than one site (dimers, or other k-mers). Such extensions would lead to new features.

Acknowledgements

We gratefully acknowledge support of this work by the US Department of Energy, Division of Chemical Sciences, Office of Basic Energy Sciences, under Grant No. DE-FG02-03ER15474, CONICET of Argentina and CONACYT of México.

Appendix

The probabilities involved in the calculation of enantioselectivity, Eqs. (19) and (21), are presented below:

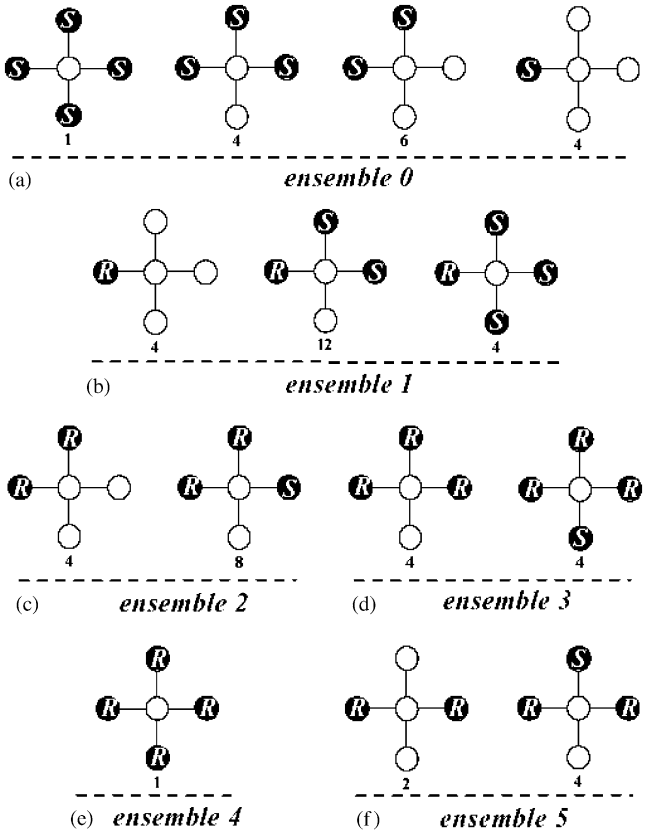

Fig. 9. (a–f) Diagrams for the calculation of probabilities $P_{R,s,i}$, for each selective ensemble.

Ensemble 0 (Fig. 9a):

$$P_{R,s,0} = \theta_A^4(1-f_{AR})^4 + 4\theta_A^3(1-f_{AR})^3(1-\theta_A) + 6\theta_A^2(1-f_{AR})^2(1-\theta_A)^2 + 4\theta_A(1-f_{AR})(1-\theta_A)^3 \,. \tag{A.1}$$

Ensemble 1 (Fig. 9b):

$$P_{R,s,1} = 4\theta_A f_{AR}(1-\theta_A)^3 + 12\theta_A^3 f_{AR}(1-f_{AR})^2(1-\theta_A) + 4\theta_A^4 f_{AR}(1-f_{AR})^3 \,. \tag{A.2}$$

Ensemble 2 (Fig. 9c):

$$P_{R,s,2} = 4\theta_A^2 f_{AR}^2(1-\theta_A)^2 + 8\theta_A^3 f_{AR}^2(1-f_{AR})(1-\theta_A) \,. \tag{A.3}$$

Ensemble 3 (Fig. 9d):

$$P_{R,s,3} = 4\theta_A^3 f_{AR}^3(1-\theta_A) + 4\theta_A^4 f_{AR}^3(1-f_{AR}) \,. \tag{A.4}$$

Ensemble 4 (Fig. 9e):

$$P_{R,s,4} = \theta_A^4 f_{AR}^4 \,. \tag{A.5}$$

Ensemble 5 (Fig. 9f):

$$P_{R,s,5} = 2\theta_A^2 f_{AR}^2 (1-\theta_A)^2 + 4\theta_A^3 f_{AR}^2 (1-f_{AR})(1-\theta_A) \,. \tag{A.6}$$

References

[1] Y. Orito, S. Imai, S. Niwa, N.G. Hung, J. Synth. Org. Chem. Japan 37 (1979) 173.
[2] S. Niwa, S. Imai, Y. Orito, J. Chem. Soc. Japan (1982) 137.
[3] J.L. Margitfalvi, M. Hegedus, J. Mol. Catal. A 107 (1996) 281.
[4] J.L. Margitfalvi, E. Tfirst, J. Mol. Catl. A 139 (1999) 81.
[5] A. Baiker, J. Mol. Catal. A 115 (1997) 473.
[6] C. LeBlond, J. Wang, J. Liu, A.T. Andrews, Y.K. Sun, J. Am. Chem. Soc. 121 (1999) 4920.
[7] T. Bürgi, A. Baiker, J. Am. Chem. Soc. 120 (1998) 12920.
[8] T. Bürgi, A. Baiker, J. Catal. 194 (2000) 445.
[9] T.J. Hall, J.E. Halder, G.J. Hutchings, R.L. Jenkins, P. Johnston, P. McMorn, P.B. Wells, R.P.K. Wells, Top. Catal. 11 (2000) 351.
[10] J. Kubota, F. Zaera, J. Am. Chem. Soc. 123 (2001) 11115.
[11] J.M. Bonello, R. Lindsay, A.K. Santra, R.M. Lambert, J. Phys. Chem. B 106 (2002) 2672.
[12] M.O. Lorenzo, C.J. Baddeley, C. Muryn, R. Raval, Nature 104 (2000) 376.
[13] A.M.M. Barbosa, P. Sauet, J. Am. Chem. Soc. 123 (2001) 6639.
[14] T.E. Jones, C.J. Baddeley, Surf. Sci. 513 (2002) 453.
[15] V. Humblot, S. Haq, C. Muryn, W.A. Hofer, R. Raval, J. AM. Chem. Soc. 124 (2002) 503.
[16] S.P. Ge, X.Y. Zhao, Z. Gai, R.G. Zhao, W.S. Yang, Chinese Phys. 11 (2002) 839.
[17] R.L. Toomes, J.H. Kang, D.P. Woodruff, M. Polcik, M. Kittel, J.T. Hoeft, Surf. Sci. Lett. 522 (2003) L9.
[18] E.M. Marti, S.M. Barlow, S. Haq, R. Raval, Surf. Sci. 501 (2002) 191.
[19] D. Stacchiola, L. Burkholder, W.T. Tysoe, J. Am. Chem. Soc. 124 (2002) 8984.
[20] F. Romá, D. Stacchiola, G. Zgrablich, W.T. Tysoe, J. Chem. Phys. 118 (2003) 6030.
[21] M. Jacoby, C& EN 80 (2002) 43.
[22] R. Raval, CATECH 5 (2001) 12.
[23] Y. Izumi, Adv. Catal. 32 (1985) 215.
[24] M.A. Keane, Langmuir 13 (1997) 41.
[25] C. LeBlond, J. Wang, J. Liu, A.T. Andrews, Y.K. Sun, J. Am. Chem. Soc. 121 (1999) 4920.
[26] J.W. Evans, Rev. Mod. Phys. 65 (1993) 1281.
[27] D. Stacchiola, M. Ciacera, C. Zuppa, T. Eggarter, G. Zgrablich, J. Chem. Phys. 108 (1998) 1730.
[28] K. Binder, Monte Carlo Methods in Statistical Physics, Springer, Berlin, 1986.